

Kinetic, isotherm and thermodynamic studies of the adsorption of phenol and tyrosine onto apatitic tricalcium phosphate

Abdelhadi El Rhilassi^{a,b*}, Nouhaila Ferraa^b and Mounia Bennani-Ziatni^b

^aTraining Center of Education Inspectors (CFIE) of Rabat, Morocco

^bLaboratory of Organic Chemistry, Catalysis and Environment, Department of Chemistry, Faculty of Sciences, Ibn Tofail University, BP 242, 14000, Kenitra, Morocco

CHRONICLE

Article history:

Received March 20, 2023

Received in revised form

June 17, 2023

Accepted October 9, 2023

Available online

October 12, 2023

Keywords:

Apatitic, Phenol

Tyrosine

Kinetic

Isotherm

Thermodynamic

ABSTRACT

The present study was conducted to evaluate the feasibility of apatitic tricalcium phosphate with a Ca/P ratio of 1.50 for the adsorption of phenol and tyrosine from aqueous solutions. The adsorbent was synthesized at room temperature using an aqueous double decomposition method and characterized through physicochemical methods. Batch adsorption studies were conducted as a function of contact time, initial adsorbate concentration, temperature, and pH. The adsorption kinetics of phenol and tyrosine were well fitted to the pseudo-second-order model. The maximum adsorption capacity was found to be 5.56 mg/g for phenol and 9.65 for tyrosine mg/g at 298 K. The adsorption of phenol and tyrosine was well explained using the Langmuir, Freundlich, Temkin, and Dubinin-Radushkevick models. The Langmuir model is the most suitable, with a maximum monolayer adsorption capacity of 7.32 mg/g for phenol and 11.43 mg/g for tyrosine at 298 K. The thermodynamic parameters indicate that the adsorption process is favorable, spontaneous, exothermic, and controlled by physisorption with electrostatic interactions between compounds containing the phenolic group and apatite. The results of this study have demonstrated the potential utility of apatitic tricalcium phosphate, which could be developed into a viable technology for the adsorption of compounds containing the phenolic group from aqueous solutions.

© 2024 by the authors; licensee Growing Science, Canada.

1. Introduction

Phenols, being organic compounds, stand out as some of the most dangerous pollutants found in the environment. Their presence is pervasive, especially in the effluents discharged from numerous industrial sectors, including chemical, petrochemical, pharmaceutical, pesticide, textile, and paper industries. Phenolic pollutants are frequently encountered in natural water bodies such as rivers, marine environments, and industrial discharges.

In light of the escalating environmental concerns, the imperative of developing effective techniques for decontaminating polluted sites has become essential. Among these techniques, adsorption emerges as a standout choice due to its widespread use, high efficiency, cost-effectiveness, resilience, ecological compatibility, and simplicity.

This process entails the use of porous materials, which can be either natural or synthetic, to facilitate adsorption and subsequent desorption. The initial step in the work involves the selection of a high-performance adsorbent, a critical determinant of success.

Among the most commonly used adsorbents are those of biological origin, such as Bio-based functionalized adsorptive polymers for sustainable water decontamination,¹ coffee grounds cellulose/ sodium alginate double-network hydrogel

* Corresponding author. Tel : +212 6 62 13 13 72
E-mail address aelrhilassi@gmail.com (A. El Rhilassi)

beads,² terrestrial and marine natural fibers³ and the new alkali-modified bio-sorbents for cadmium removal from industrial discharges.⁴

Calcium phosphates have garnered substantial attention for their efficacy in adsorbing various pollutants, including heavy metal ions,⁵ nitrobenzene,⁶ fluoride,⁷ textile dye⁸ and biologically significant macromolecules like amino acids⁹ and proteins¹⁰. Natural phosphate and poorly crystalline synthetic hydroxyapatite have shown promise in removing dyes from aqueous solutions.^{11,12}

Among the calcium phosphates, apatites, in particular, have emerged as materials of remarkable interest. They possess desirable attributes such as abundant availability, ion exchange capabilities, strong adsorption affinity, and the ability to form bonds with organic molecules of varying sizes. These characteristics have elevated the significance of apatitic materials in environmental remediation. Further accentuating the appeal of poorly crystallized apatites is their surface reactivity, which bears a striking resemblance to the physicochemical properties of bone minerals.^{13,14} Their excellent biocompatibility, slow biodegradability, osteoconductivity, and mechanical strength have ignited interest in their application beyond environmental remediation.

In this article, we delve into a comprehensive exploration of the adsorption behavior of organic compounds, specifically phenol and the phenolic amino acid tyrosine, onto calcium phosphate in the form of apatitic tricalcium phosphate, characterized by a Ca/P atomic ratio of 1.50. The adsorption studies were carried out under various experimental conditions, such as pH, contact time, initial adsorbate concentrations, and temperature.

To elucidate the adsorption process, we employ diverse kinetic models, including the pseudo first order, the pseudo second order, the Elovich equation, and the intraparticle diffusion model of Weber and Morris. The Langmuir, Freundlich, Temkin, and Dubinin–Kaganer–Radushkevich (D–K–R) models are used to describe equilibrium isotherms. Additionally, we calculate kinetic and thermodynamic parameters to provide a comprehensive understanding of the adsorption mechanism of phenol and tyrosine compounds on apatitic tricalcium phosphate.

The ensuing discussion of our findings promises to shed valuable light on the intricacies of phenol and tyrosine adsorption onto apatitic tricalcium phosphate, contributing to our broader comprehension of this environmental remediation process.

2. Materials and methods

2.1 Preparation of the adsorbent (PTCa)

The apatitic tricalcium phosphate (PTCa) is synthesized at room temperature by an aqueous double decomposition method. We add quickly the solution A with pH ~11.2 (47 g of calcium nitrate $\text{Ca}(\text{NO}_3)_2 \cdot 4\text{H}_2\text{O}$ (from Scharlau, Spain) in 550 ml of distilled water + 20 ml of ammonia solution) into the solution B with pH~9.9 (26 g of di-ammonium hydrogen phosphate $(\text{NH}_4)_2\text{HPO}_4$ (Riedel-de Haën, Germany) in 1300 ml of distilled water + 20 ml ammonia solution).

The formed precipitate is filtered by pyre, washed with 3000 ml of distilled water containing 15 ml of ammonia solution and dried at 80 °C for 24 hours.

2.2 Characterization of the adsorbent (PTCa)

2.2.1 Chemical Analyse

The phosphate ion content in the solid is determined by spectrophotometry (GBC UV Visible spectrophotometer 911A at 460 nm) using phospho-vanado-molybdic acid and calcium ion content by complexometry with Ethylene Diamine Tetra Acetic Acid (EDTA). The mean values of the quantity of calcium and phosphate ions are $8.65 \pm 0.05\text{mmol}$ and $5.78 \pm 0.05\text{mmol}$, respectively. The mean value obtained of Ca/P molar ratio of powder is 1.50 ± 0.01 , which indicates the synthesis of apatitic tricalcium phosphate (PTCa) of formula : $\text{Ca}_9(\text{HPO}_4)(\text{PO}_4)_5(\text{OH})$

2.2.2 Surface Area

The specific surface area of apatitic tricalcium phosphate synthesised is $62 \pm 3 \text{ m}^2/\text{g}$ with an error of 5 %, it's determined by BET (Brunauer, Emmett, and Teller) method using N_2 adsorption.

2.2.3 Point of zero charge determination pH_{ZPC} of PTCa

The zero-point charge is determined using a simple technique. 20mL of 0.01 M NaCl solution is added to a series of beakers containing 0.2 g of apatite powder, the initial pH_i is adjusted by using NaOH (0.1 M) or HCl (0.1 M) solution in the range of 4–10. After 48 hours of stirring speed (250 rpm) at ambient temperature, the final pH_f is measured, the difference

$\Delta pH = pH_i - pH_f$ is plotted against the initial pH_i . pH_{ZPC} is determined by intersection of the axis $pH_i = pH_f$ with ΔpH . The pH_{ZPC} of PTCa prepared at room temperature is found approximately 5.6 (Fig.1).

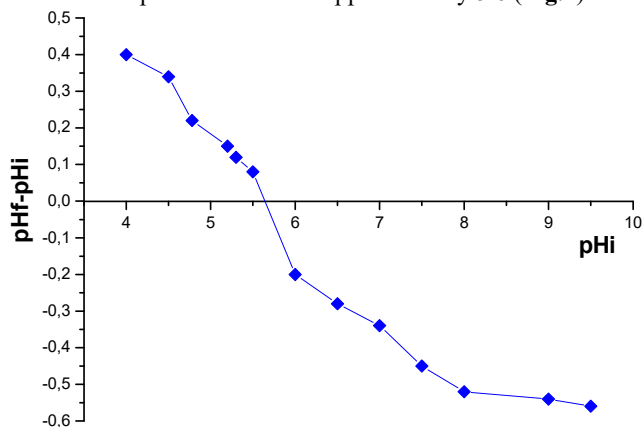


Fig. 1. pH_{ZPC} of PTCa

2. 2. 4 X-Ray Diffraction Pattern of PTCa

XRD of the TCPa powder is analyzed using X-ray diffractometer (Siemens D-500, Germany) with Cu Ka radiation. Fig. 2 shows the peaks of broad and overlapping reflections, indicating phase with low crystallinity of apatite studied.

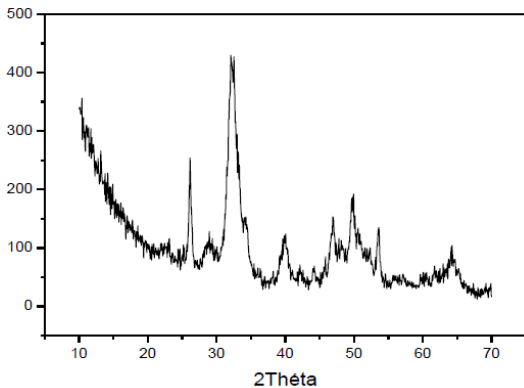


Fig. 2. XRD pattern of the PTCa precipitate at room temperature

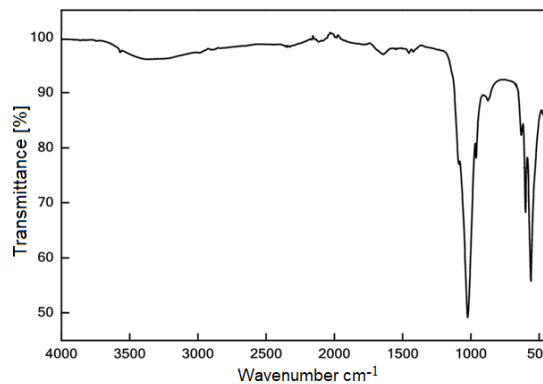


Fig. 3. FTIR spectrums of PTCa precipitate at room temperature

2. 2. 5 Infrared spectrum

The FT-IR is accomplished after dispersion of anhydrous KBr (2 mg solid to 200 mg of KBr) using VERTEX 70 spectrophotometer (Bruker Optics, Germany) (Fig. 3). The absorption bands appear at 3570 and 634 cm^{-1} are attributed to the OH^- group. The peaks at 1030, 962, 603 and 565 cm^{-1} are assigned to the P-O stretching and bending vibration of the PO_4^{3-} group. The band located at 675 cm^{-1} associated with HPO_4^{2-} ions due to the stretching vibration of the link $PO(H)$, confirms that it is a deficient apatite. The most characteristic chemical groups are given in Table 1.

Table 1. FTIR absorption peak positions of prepared PTCa and their corresponding assignments.¹⁵

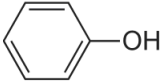
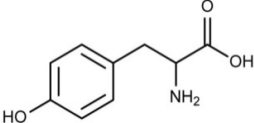
Peak position, cm^{-1}	Corresponding assignment
3570 ; 634	OH^-
875	HPO_4^{2-}
1030 ; 960 ; 603 ; 565	PO_4^{3-}

2.3 Adsorbates

The adsorbates used in this work are phenol and tyrosine. Both organic compounds contain an aromatic ring in the presence of a hydroxy group. The phenol is also known as carbolic acid, it's used as anesthetic, disinfectant, antiseptic, household cleaning products and as starting material or produce as an intermediate in industry. The tyrosine is not essential, it is synthesized in the human body from another essential amino acid, phenylalanine, it can be found in certain foods such as fish, meat, eggs, dairy products, bananas, pumpkin, almonds, oats, wheat...etc. The characteristics and properties of these adsorbates are illustrated in Table 2.

The Infrared absorption spectra of phenol and tyrosine in 4000–400 cm^{-1} region is shown in **Fig.4** and **5**. The most characteristic chemical groups of these adsorbates are given in **Table 3**.

Table 2. Physicochemical properties of phenol and tyrosine.

Adsorbate	phenol	tyrosine
Chemical structure		
Molecular formula	$\text{C}_6\text{H}_6\text{O}$	$\text{C}_9\text{H}_{11}\text{NO}_3$
Acidity (pKa)	9,95	2,2 (carboxyl), 9,11 (amino), 10,07 (phenol group)
Molecular weight (g/mol)	94,11	181,19
Isoelectric point (pI)	-	5,66
Solubility in water at 25°C (g/L)	76,04	0,48

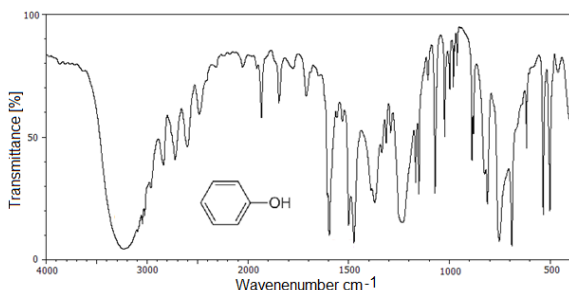


Fig. 4. Infrared absorption spectrum of phenol

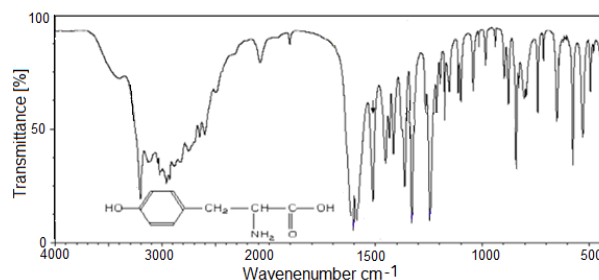


Fig. 5. Infrared absorption spectrum of tyrosine

Table 3. FTIR absorption bands of phenol and tyrosine chemical groups.

phenol		tyrosine	
Chemical groups	Absorption bands, (cm^{-1})	Chemical groups	Absorption bands, (cm^{-1})
O-H	3220	N-H	3400;1609;1591
C=C	1500	O-H	3203; 3300 -2500
C-O	1240	C-H	803; 1591
C-H	812 ; 1598	C=C	1513
		C-N	1250-1360

2.4 Experimental protocol

The adsorption experiments were carried out in thermostatic bath at room temperature (298K) and neutral pH (7) of different contact times. We added 10 ml of adsorbate to a test tube containing 200 mg of apatitic tricalcium phosphate powder (PTCa) of Ca/P ratio 1.50. The mixture was agitated at fixed contact time (2min) and at 1000 trs/min. The solid was separated from the solution by filtration using a sintered glass N°4 and dried in an oven at 80°C overnight.

The supernatants obtained are examined by measuring the pH and determining the equilibrium concentration using a UV-vis spectrophotometer (ZUZI Model 4201/50, Japan) at 511 nm for the phenol and 570 nm for the Tyrosine.

The adsorption capacity of adsorbate adsorbed was evaluated by following formula:

$$q_{ads}(\text{mg/g}) = V(C_0 - C)/m \quad (1)$$

where $C_0(\text{mg/g})$ is the initial adsorbate concentration, $C(\text{mg/g})$ is the concentration of adsorbate at equilibrium time, $V(l)$ is the solution volume and $m(\text{g})$ is the adsorbent mass in contact with adsorbate solution.

3. Results and discussion

3.1 Adsorption kinetics

The adsorption kinetics was investigated with initial adsorbate concentration 200 mg/L at 298K and pH neutral solution. Experimental result of adsorption of phenol and tyrosine on apatitic tricalcium phosphate of Ca/P=1.50 at contact time (0, 15, 30, 60, 180, 300, 480, 1080, 1440min) was reported in **Fig. 6**. The adsorption kinetics is fast, the equilibrium is reached

after about 180 min of incubation for phenol and 300 min for tyrosine. The maximum adsorption is noted in the first minutes of contact, due to the high number of active sites available at the beginning of adsorption process. The formation of plateaux a few minutes indicates that the phosphate in dispute is very effective adsorbent. The highest quantity absorbed is obtained for tyrosine; polar amino acid. From **Fig. 6**, the maximum adsorbed amounts of phenol and tyrosine are 5.56 mg/g and 9.65 mg/g, respectively.

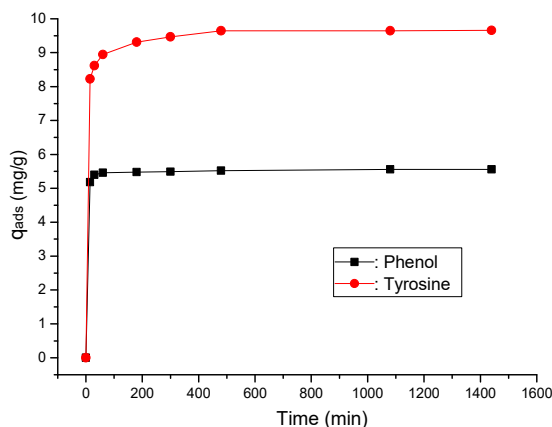


Fig. 6. Adsorption kinetics of phenol and tyrosine on PTCa ($C_0 = 200$ mg/l)

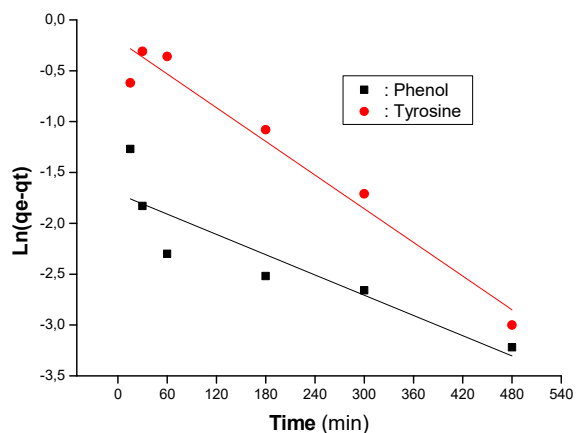


Fig. 7. Pseudo-first-order kinetic model for the adsorption of phenol and tyrosine onto PTCa

To fully understand the kinetics data of phenol and tyrosine adsorption by apatitic tricalcium phosphate, four simplified kinetic models, namely the pseudo first order¹⁶, the pseudo second order¹⁷, the Elovich equation¹⁸, the intraparticle diffusion model of Weber and Morris¹⁹ are studied, evaluated and their parameters have been determined.

3.1.1 pseudo-first-order model

The pseudo first order kinetics model is described by the Lagergren equation:

$$dq_t/dt = K_1(q_e - q_t) \quad (2)$$

The integration of this equation leads to the following linear form:

$$\ln(q_e - q_t) = \ln q_e - K_1 t \quad (3)$$

where, q_t ($mg\ g^{-1}$) and q_e ($mg\ g^{-1}$) are the amount of adsorbate adsorbed at any time t (min) and at equilibrium on PTCa, respectively. K_1 (min^{-1}) represents the equilibrium rate constant of pseudo first order reaction.

The constant K_1 and theoretical equilibrium adsorption capacity q_e (Cal) determined from straight-line plot of $\ln(q_e - q_t)$ versus t (**Fig.7**) at 298 K, are given in **Table 4**. The values of the calculated q_e (Cal) and the experimental q_e (exp) for the two adsorbates are very different. In addition, the values of the correlation coefficient R^2 are less than unity. Therefore, the adsorption of the phenol and tyrosine on PTCa does not follow the pseudo-first-order kinetic model.

3.1.2 Pseudo-second order model.

The pseudo second order model is described by Ho and McKay equation:

$$dq_t/dt = K_2(q_e - q_t)^2 \quad (4)$$

The integration of this equation leads to the following linear form:

$$t/q_t = 1/K_2 \cdot q_e^2 + t/q_e \quad (5)$$

K_2 ($g/mg \cdot min$) represents the equilibrium rate constant of pseudo second order reaction. The values of q_e (Cal) and K_2 (**Table 4**) are calculated from the slopes and intercepts of the linear plots obtained by plotting t/q_t against t (**Fig.8**).

Calculated q_e (cal) and experimental q_e (exp) values are nearly equal for each of the phenol and tyrosine adsorbates. The correlation coefficient ($R^2 > 0.999$) for the two adsorbates is very high and close to unity. These results show that the pseudo-second order kinetic model is suitable to explain the adsorption reaction of phenol and tyrosine on PTCa.

The initial adsorption rate g ($mg/g \text{ min}$), is calculated at $t \rightarrow 0$ from the following relation :

$$g = K_2, q_e^2 \quad (6)$$

The values obtained of g (**Table 4**), show that the phenol has an initial adsorption reaction rate (2.642 mg/g.min) almost higher than that of the tyrosine (2.373 mg/g.min). In the same way, we note that the constant of the adsorption rate K_2 for phenol (0.0853 g/mg.min) is higher than that of tyrosine (0.0253 g/mg.min), this can be explained by the fact that the composition and the functional groups of the two adsorbates are quite different.

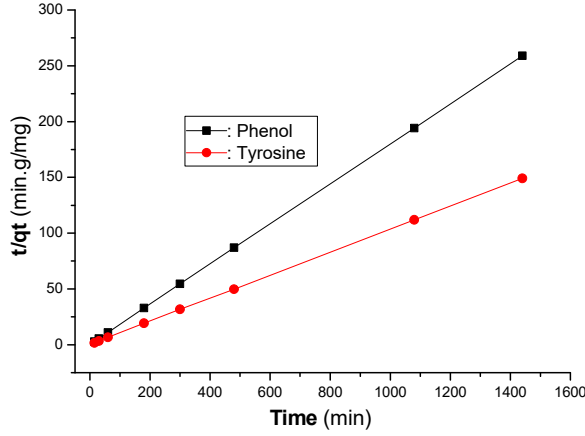


Fig. 8. Pseudo second order kinetic model for the adsorption of phenol and tyrosine onto PTCa

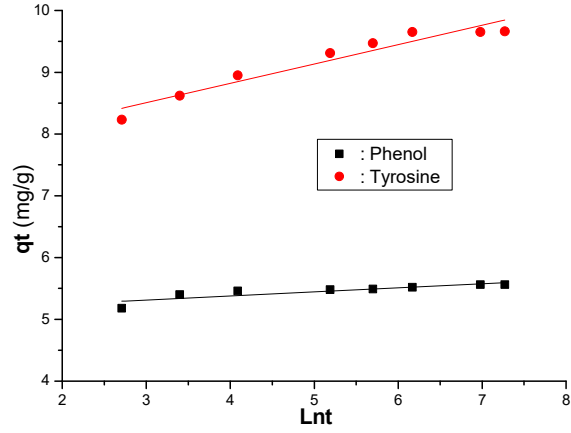


Fig. 9. Plot of Elovich equation for adsorption of phenol and tyrosine onto PTCa

3.1.3 Elovich kinetic model

The kinetic expression of the Elovich model is described by Chien and Clayton equation:

$$dq_t/dt = \alpha, \exp(-\beta, q_t) \quad (7)$$

The integration of this equation leads to the following linear form:

$$q_t = Ln(\alpha, \beta)/\beta + Ln(t)/\beta \quad (8)$$

where, α ($mg/g.h$) and β (g/mg) are the initial adsorption constant rate and the desorption constant during the adsorption process, respectively. These constants are determined from the slope and intercept of the linearized plot of q_t versus $Ln t$ (**Fig.9**) and are summarized in **Table 4**.

We note that α and β constants are very different (**Table 4**), and depends to the adsorbate type; indeed, the initial adsorption rate and the desorption constants are much higher for phenol than that of the tyrosine. This finding may be explained by the composition and the functional groups of the two adsorbates which are quite different. The correlation coefficients R^2 corresponding to phenol (0.736) and tyrosine (0.920) are lower than pseudo-second order model. These results show that the Elovich kinetic model could not be suitable to explain the adsorption reaction of phenol and tyrosine on PTCa.

3.1.4 Intra-particle diffusion model

The kinetic expression of the intra-particle diffusion model is described by Weber and Morris equation :

$$q_t = K_p t^{1/2} + C \quad (9)$$

where, C represent the constant indicative of the boundary layer thickness effect and K_p ($mg.g^{-1}.min^{1/2}$) represent the rate constant for intra-particle diffusion model. These parameters are calculated from the plot of q_t versus $t^{1/2}$ (**Fig.10**) and given in **Table 4**.

The K_p and C constants values are influenced by the type of adsorbate; they are important for tyrosine. In addition, the values constants C corresponding to phenol and tyrosine are not null and almost equal to the quantities values found experimentally in the case of second-order kinetics.

Table 4. Parameters for various kinetic models for phenol and tyrosine adsorption on PTCa at 298 K.

Kinetic models	Parameters	Phenol	Tyrosine
Pseudo-first order	$K_1 (min^{-1})$	$3.32 \cdot 10^{-3}$	$5.53 \cdot 10^{-3}$
	$q_e(cal) (mg/g)$	0.181	0.820
	$q_e(exp) (mg/g)$	5.56	9.65
	$R^2 (\%)$	0.757	0.952
Pseudo-second order	$K_2 (g/mg \cdot min)$	$8.528 \cdot 10^{-2}$	$2.529 \cdot 10^{-2}$
	$q_e(cal) (mg/g)$	5.566	9.689
	$q_e(exp) (mg/g)$	5.56	9.65
	$g (mg/g \cdot min)$	2.642	2.373
	$R^2 (\%)$	0.999	0.999
Elovich	$\beta (g/mg)$	15.295	3.188
	$\alpha (mg/g \cdot min)$	$6.39 \cdot 10^{32}$	$9.25 \cdot 10^9$
	$R^2 (\%)$	0.736	0.920
Intra-particle diffusion	$K_p (mg \cdot g^{-1} \cdot min^{0.5})$	$7.43 \cdot 10^{-3}$	$3.62 \cdot 10^{-2}$
	$C (mg/g)$	5.325	8.556
	$R^2 (\%)$	0.507	0.671

The values of the regression coefficient R^2 are between 0.51 and 0.67, probably indicating that intra-particle diffusion is not a rate-limiting step for the adsorption rate throughout the time. However, the graph of **Fig.10** is not linear, it shows a multi-linearity with three different adsorption steps. The first (1) between 15 and 60 min is instantaneous adsorption on the external surface of the solid. The second (2) between 60 and 480 min is the gradual adsorption stage where intraparticle diffusion is limited and the third stage (3) between 480 and 1440 min is the final stage where intraparticle diffusion begins to slow down due to the low concentration of the solute in solution. According to **Table 5**, portion (2) is the step that presents a high correlation coefficient between 0.94 and 0.97, this may suggest that this step is the limiting step that determines the rate of progressive diffusion of phenol and tyrosine on apatitic tricalcium phosphate. In all these results, the adsorption reaction process of these adsorbates on PTCa is complex, and only the second step can control the kinetics of intraparticle diffusion.

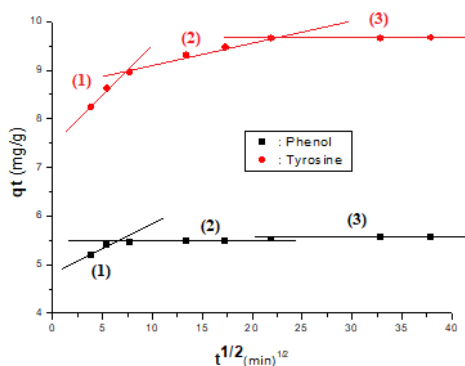


Fig. 10. Intra-particle diffusion model plot for adsorption of phenol and tyrosine onto PTCa :
(1) [15-60min] ; (2) [60-480min] ; (3) [480-1440min]

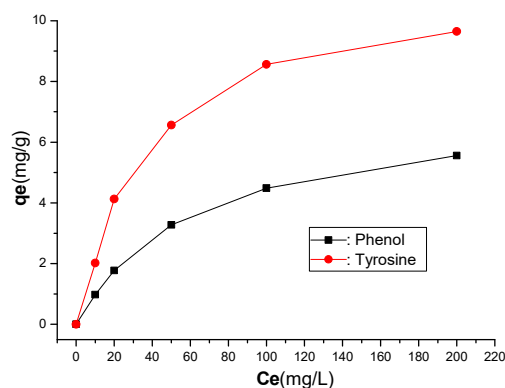


Fig. 11. Adsorption isotherms of phenol and tyrosine onto PTCa (solid quantity: 200 mg, stirring time : 1 min, T : 298 K)

Table 5. Weber and Morris model parameters and correlation coefficients for different stages.

Stage	Phenol			Tyrosine		
	$K_p (mg \cdot g^{-1} \cdot min^{0.5})$	$C (mg/g)$	R^2	$K_p (mg \cdot g^{-1} \cdot min^{0.5})$	$C (mg/g)$	R^2
(1)	0.0689	4.9546	0.6580	0.1828	7.5601	0.9519
(2)	0.00408	5.4259	0.9424	0.0491	8.603	0.9744
(3)	0.00268	5.4638	0.8076	$3.348 \cdot 10^{-4}$	9.6371	0.8076

In all the results of the four kinetic models applied to the experimental data, we find that the most suitable, the best fitted and also the most potential model used as a kinetic model of phenol and tyrosine adsorption on PTCa is that of pseudo-second order with the highest values of the regression coefficients ($R^2 > 0.999$) and give also a good correlation between the theoretical and experimental values of q_e for each of the phenol and tyrosine adsorbates. These results agree with our recently obtained results: adsorption of methionine on poorly crystalline hydroxyapatite with different Ca/P ratios⁹ and adsorption of insulin on synthetic hydroxyapatite.²⁰

3.2 Adsorption isotherms

The evolution of the amounts $q_e (mg/g)$ adsorbed of phenol and of tyrosine on apatitic tricalcium phosphate as a function of the equilibrium concentration $C_e (mg/L)$ at pH~7 and at 298 K, is represented in **Fig .11**. The adsorption isotherms are determined in contact time of 18 hours, time largely sufficient to reach equilibrium.

We find that a rapid increase in q_e for low equilibrium concentrations C_e is followed by reaching plateau; this can be explained by the fact that adsorption can be governed by the formation of a monolayer of adsorbate and that apatitic tricalcium phosphate studied could adsorb significant amounts of the adsorbate.

To properly study the phenomenon of adsorption of phenol and tyrosine onto PTCa, it is necessary to evaluate the mathematical equations that describe the experimental data of adsorption equilibria obtained. For this reason, four isothermal models have been evaluated and adjusted: the Langmuir²¹, the Freundlich²², the Temkin²³ and Dubinin–Kaganer–Radushkevich (D-K-R)²⁴.

3.2.1 Langmuir isotherm

The Langmuir adsorption model is given by the following equation:

$$q_e = q_m K_L C_e / (1 + K_L C_e) \quad (10)$$

The linear form of this model can be described by the following equation:

$$C_e/q_e = 1/K_L q_m + C_e/q_m \quad (11)$$

where C_e (mg/L) and q_e (mg/g) are the equilibrium concentration of adsorbate used and the amount of adsorbate per unit mass of apatitic tricalcium phosphate, respectively. q_m (mg/g) and K_L (L/g) are the equilibrium adsorption capacity and the Langmuir constant related to the adsorption capacity, respectively.

The representation of C_e/q_e as a function of C_e at 298 K is given in **Fig.12**. The q_m and K_L parameters of this model are calculated by linear regression from the slope and intercept, respectively, and listed in **Table 6**. The equilibrium adsorption capacity, q_m , which is a measure of the maximum adsorption capacity corresponding to complete monolayer coverage, has been influenced by the nature and chemical composition of adsorbate; its value was found to be 7.323 mg/g for the phenol and 11.428 mg/g for the tyrosine. The adsorption coefficient, K_L , value was 15,843 L/g for the phenol and 27,853 L/g for the tyrosine. Therefore, the interaction between apatitic tricalcium phosphate of Ca/P=1.50 and the adsorbate is more important for tyrosine than for phenol. In addition, the values of the correlation coefficient corresponding to the Langmuir isothermal model are very high ($R^2 > 0.999$), which justifies that this model is good for adjusting the experimental data.

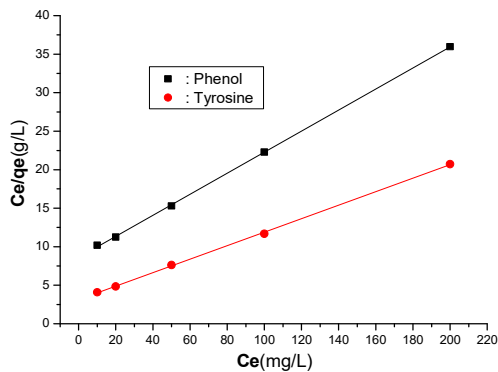


Fig. 12. Langmuir isotherm model

Table 7. Equilibrium parameter (R_L) values for phenol and tyrosine adsorption by PTCa at 298 K.

C_0 (mg/L)	R_L	
	Phenol	Tyrosine
10	0.863	0.782
20	0.760	0.643
50	0.558	0.418
100	0.631	0.264
200	0.240	0.152

The Langmuir adsorption process is linked to an equilibrium parameter denoted R_L , which makes it possible to evaluate the advantage and efficiency of this model, it is given by the following equation²⁵:

$$R_L = 1 / (1 + K_L C_0) \quad (12)$$

C_0 (mg/L) and K_L (l/g) are the initial concentration of adsorbate and the Langmuir constant, respectively.

In the literature²⁵, the R_L value indicates that adsorption is favorable when $0 < R_L < 1$, unfavorable when $R_L > 1$. In this paper, all R_L values found are less than 1 (**Table 7**), which indicates that the adsorption of phenol and tyrosine onto the surface of the apatitic tricalcium phosphate was a favorable process. The Langmuir constant, K_L , makes it possible to calculate the free energy thermodynamic parameter ΔG_{ads}^0 (J/mol) of adsorption and to evaluate the nature of the adsorption process studied at 298 K. This parameter is given by the following equation²⁶:

$$\Delta G_{ads}^0 = -R T \ln K_L \quad (13)$$

where R (8.314 J mol⁻¹ K⁻¹) is the universal gas constant and T (K) is the absolute temperature.

At 298 K, the values found of ΔG_{ads}^0 (Table 6) are negative for phenol and tyrosine and are between -20 KJ/mol and 0 KJ/mol . This result shows that the adsorption process is considered spontaneous and is often of a physical type.²⁷

3.2.2 Freundlich isotherm

The Freundlich adsorption model is given by the following equation:

$$q_e = K_F C_e^{\frac{1}{n}} \quad (14)$$

The linear form of this model can be described by the following equation:

$$\ln q_e = \ln K_F + 1/n \ln C_e \quad (15)$$

where $C_e (\text{mg/L})$ and $q_e (\text{mg/g})$ are respectively the equilibrium concentration of the adsorbate used and the quantity of adsorbate per unit mass of apatitic tricalcium phosphate. n and $K_F (\text{L/mg})$ are respectively the heterogeneity parameter relating to the adsorption intensity and the Freundlich constant relating to the adsorption capacity of the adsorbent. In the literature²⁸, the inverse of the parameter n makes it possible to give an indication of the favorable or unfavorable nature of the adsorption process; it is favorable for $0.1 < 1/n < 1$ and unfavorable for $1/n > 1$. From the plot $\ln q_e$ versus $\ln C_e$ (Fig. 13), we can calculate the slope $1/n$ and the intercept $\ln K_F$. The values of K_F , n , $1/n$ and the coefficient of determination, R^2 , are shown in Table 6. We find that the Freundlich constant K_F depends on the nature of the adsorbate used; its value was found to be 0.292 L/mg for phenol and 0.769 L/mg for tyrosine. Consequently, the interaction between the apatitic tricalcium phosphate of $\text{Ca/P}=1.50$ and the adsorbate is more important for tyrosine than for phenol. The R^2 values obtained are between 0.959 and 0.899, which shows that this model is not as good as the Langmuir isotherm model in describing the experimental data. Additionally, we see that the values of $1/n$ are less than one ($1/n < 1$), indicating that adsorption processes tend to be favorable.

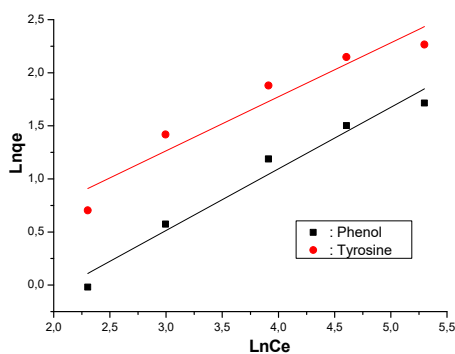


Fig. 13. Freundlich isotherm model

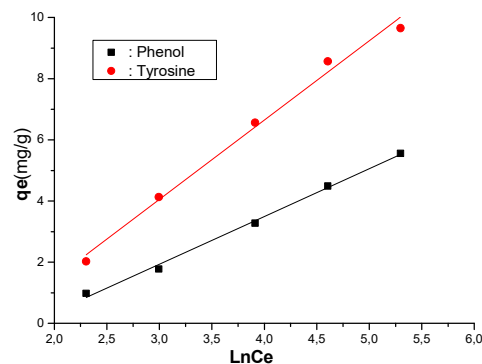


Fig. 14. Temkin isotherm model

3.2.3 Temkin isotherm

The Temkin adsorption model is given by the following equation:

$$q_e = (R T/b_t) \ln a_t C_e \quad (16)$$

This equation can be expressed in its linear form as:

$$q_e = (R T/b_t) \ln a_t + (R T/b_t) \ln C_e \quad (17)$$

where $R (8.314 \text{ J mol}^{-1} \text{ K}^{-1})$ and $T (298 \text{ K})$ are the universal gas constant and the temperature, respectively. $C_e (\text{mg/L})$ and $q_e (\text{mg/g})$ are respectively the equilibrium concentration of the adsorbate used and the quantity of adsorbate per unit mass of apatitic tricalcium phosphate.

$a_t (\text{L/mg})$ and $b_t (\text{J/mol})$ are the Temkin isotherm constants associated with the maximum binding energy and the heat of adsorption, respectively. These Temkin constants are determined from the slope and intercept of the plot of q_e versus $\ln C_e$ (Fig. 14) and are given in Table 6. The R^2 values of the Temkin model are between 0.989 and 0.995, they are almost higher than the values of the Freundlich model, but they are almost lower than those of the Langmuir model, which suggests that the Temkin model which is between Freundlich and Langmuir can be satisfied experimental data. It is interesting to note that Temkin's constant a_t depends on the nature of the adsorbate studied, its value is of the order of 0.171 L/mg for phenol and 0.237 L/mg for tyrosine. This is the same observation as for the Langmuir constant K_L and the Freundlich constant K_F . We also note that the values of b_t obtained are between 0.954 and 1.585 KJ/mol . They are weak and positive, indicating that the adsorption processes are exothermic and can be considered purely electrostatic.

3.2.4 Dubinin–Kaganer–Radushkevich (D-K-R) isotherm

The Dubinin–Kaganer–Radushkevich isotherm model is represented by the empirical equation below:

$$q_e = q_D \exp(-B_D \mathcal{E}^2) \quad (18)$$

where q_e (mg/g) and q_D (mg/g) are respectively the amount of adsorbate per unit mass of adsorbent and the maximum adsorption capacity representing the total specific micropore volume of the adsorbent.

The \mathcal{E} is the Polanyi potential can be calculated as:

$$\mathcal{E} = R T \ln(1 + 1/C_e) \quad (19)$$

where C_e (mg/L), R (8.314 J mol⁻¹ k⁻¹) and T (298 k) are respectively the equilibrium concentration of the adsorbate used, the universal gas constant and the temperature.

The D-K-R model constant, B_D (mol/KJ)², is related to mean adsorption free energy E (J/mol) per molecule of adsorbate as it migrates to the surface of the adsorbent from infinite distance in the solution. B_D and E are linked by the following expression:

$$E = 1/\sqrt{2 B_{DR}} \quad (20)$$

The linearized form of Eq. (18) is given as follows:

$$\ln q_e = \ln q_D - B_D \mathcal{E}^2 \quad (21)$$

The plot of $\ln q_e$ versus \mathcal{E}^2 gives B_D and q_D (**Fig. 15**). The values of all parameters of this model are listed in **Table 6**. We noted that the adsorption capacity is greater for tyrosine (14.437 mg/g) than for that of phenol (8.157 mg/g). This is in close agreement with the results regarding q_m values obtained for the Langmuir isotherm model.

Table 6. Values of the parameters of Langmuir, Freundlich, Temkin and Dubinin–Kaganer–Radushkevich models for the adsorption of phenol and tyrosine on apatitic tricalcium phosphate of Ca/P=1.50 at 298 k.

Models	Parameters	Phenol	Tyrosine
Langmuir	K_L (L/g)	15.843	27.853
	q_m (mg/g)	7.323	11.428
	R^2 (%)	0.9998	0.9995
	ΔG_{ads}^0 (KJ/mol)	-7.121	-8.574
Freundlich	K_F (L/mg)	0.292	0.769
	$1/n$	0.581	0.5092
	n	1.721	1.964
	R^2 (%)	0.9593	0.8999
Temkin	b_t (KJ/mol)	1.585	0.954
	a_t (L/mg)	0.171	0.237
	R^2 (%)	0.9951	0.9888
Dubinin–Kaganer–Radushkevich (D-K-R)	E (KJ/mol)	5.573	5.895
	B_D (mol/KJ) ²	0.0161	0.0144
	q_D (mg/g)	8.157	14.437
	R^2 (%)	0.9998	0.9808

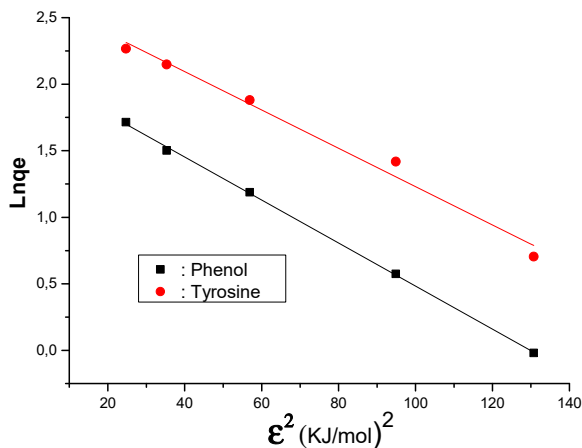


Fig. 15. Dubinin–Kaganer–Radushkevich isotherm model

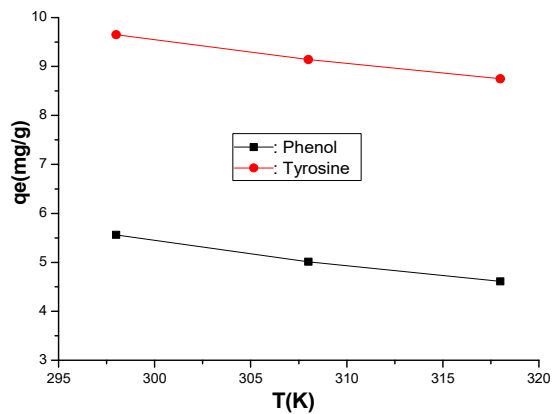


Fig. 16. Effect of temperature on the equilibrium adsorption of phenol and tyrosine on PTCa (Solid quantity: 200 mg, initial adsorbate concentration: 200 mg/L, initial pH, stirring time: 1 min, contact time: 18 h).

In the literature²⁹, the energy E is used to describe the type of adsorption; if E is between 1.0 and 8.0 KJ/mol, the adsorption is physical and if E is between 9.0 and 16.0 KJ/mol, the adsorption is chemical. In this work, we found that the values of E are between 1.0 and 8.0 KJ/mol (**Table 6**) which indicates that the adsorption of phenol and tyrosine onto apatitic tricalcium phosphate of Ca/P=1.50 at 298 k may be attributed to the physical adsorption. We also noted that the coefficient of regression, R^2 , value is almost equal to the value of the Temkin model.

From the analysis of all the parameters of the results listed in **Table 6**, it appears that the Langmuir model is the most suitable isotherm compared to the Freundlich, Temkin and Dubinin-Radushkevich models for fitting the equilibrium experimental data adsorption of phenol and tyrosine on apatitic tricalcium phosphate of Ca/P=1.50 at 298 k. These results agree with our recently obtained results: interaction of insulin with apatitic calcium phosphates³⁰, adsorption of insulin on synthetic hydroxyapatite²⁰ and adsorption of methionine on poorly crystalline hydroxyapatite with different Ca/P ratios.⁹

3.3 Effect of temperature on adsorption equilibrium and thermodynamic parameters

In this part, we are interested in the influence of temperature on the adsorption of two different molecules such as phenol and tyrosine on apatitic tricalcium phosphate (PTCa) of Ca/P=1.50. For this reason, three temperatures are tested: 298 K, 310 K and 318 K. The plot $q_e(mg/g)$ versus $T(k)$ (**Fig. 16**) is obtained for a period of 18 hours, for an initial concentration $C_0 = 200 mg/L$ of adsorbate and for a neutral pH. The results show that increasing the temperature leads to a decrease in the equilibrium adsorbed quantity of adsorbate.

In order to understand the effect of temperature on the adsorption process between phenol, tyrosine and PTCa, it is necessary to determine thermodynamic parameters such as ΔG , ΔH and ΔS . These parameters were calculated using the following standard thermodynamic Relationship:^{31,32}

$$K_C = (C_0 - C_e)/C_e \quad (22)$$

$$\Delta G = -RT \ln K_C \quad (23)$$

$$\Delta G = \Delta H - T\Delta S \quad (24)$$

where $C_0(mg/L)$ and $C_e(mg/L)$ are respectively the initial and equilibrium concentration of the methionine in solution. $R(8.314 J mol^{-1} k^{-1})$ and $T(k)$ are respectively the universal gas constant and the temperature. K_C is the thermodynamic equilibrium constant. $\Delta G(J/mol)$, $\Delta H(J/mol)$ and $\Delta S(J/mol k)$ are respectively the change in Gibbs free energy, the change in enthalpy and the change in entropy.

The Gibbs free energy change ΔG is calculated at different temperatures from relation (23) and the parameters values of ΔS and ΔH are determined respectively from the slopes and origins of the plots of ΔG in the function of T which are linear (**Fig. 17**), the values of the regression coefficients R^2 are greater than 0.99. The values of all thermodynamic parameters are collected in **Table 8**.

The results obtained show that the free energy (ΔG) values are all negative at each temperature, which indicates the feasibility and spontaneous nature of the adsorption of phenol and tyrosine on PTCa of Ca/P= 1.50. Also note that these values decrease slightly when the temperature increases from 298 k to 318 k, which suggests that the adsorption process is unfavorable with an increase in temperature. In addition, these values are also between -20 and 0 kJ/mol which indicates the processes adsorption of phenol and tyrosine on PTCa can be physical adsorption.³³ This is in agreement with the parameter values obtained from the Langmuir quantities ΔG_{ads}^0 .

The negative values of the parameter ΔS which are between $-3.80 J/mol k$ and $-23.65 J/mol k$ show a disorder that is established on the surface of the PTCa apatite with respect to the phenol and tyrosine molecules during the adsorption process.³⁴ According to Table 8, the parameter ΔS becomes less negative going from the phenol to the tyrosine molecule. This also indicates that the disorder increases with the size and nature of the functional group present in the adsorbed molecule.

The negative values of the ΔH parameter obtained in this study ($-8.271 < \Delta H(kJ/mol) < -15.771$) showed that the adsorption processes were exothermic in nature and the low values of this parameter suggest that the adsorption processes may be pure physisorption.³⁵ These results agree with those recently obtained in previous work.⁹

Table 8. Thermodynamic parameters of adsorption of phenol and tyrosine on PTCa.

Adsorbate	$T(K)$	$\Delta G(kJ/mol)$	$\Delta H(kJ/mol)$	$\Delta S(J/mol k)$	$R^2(\%)$
Phenol	298	-7.138	-8.271	-3.80	0.998
	310	-7.102			
	318	-7.062			
Tyrosine	298	-8.723	-15.771	-23.65	0.999
	310	-8.488			
	318	-8.250			

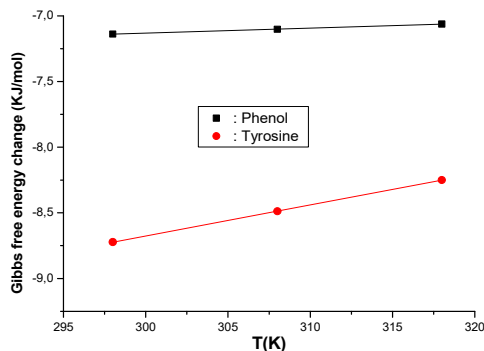


Fig. 17. Van't Hoff plot

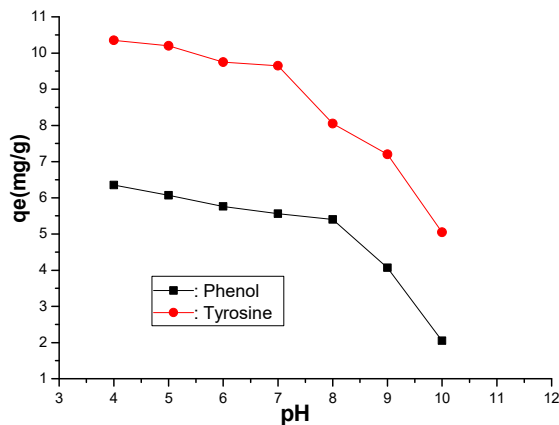


Fig. 18. Effect of pH on the adsorption of phenol and tyrosine on PTCa (solid quantity: 200 mg, initial adsorbate concentration: 200 mg/L, stirring time: 1 min, contact time: 18 h)

3.4 Effect of pH on the adsorption of phenol and tyrosine

The effect of pH was studied by adding 200 mg of PTCa into test tubes containing 10 ml of the adsorbate solutions (phenol and tyrosine). The initial concentrations of phenol and tyrosine solutions were set at 200 mg/L, for all batch experiments. The study is carried out in an initial pH range between 4 and 10. The mixtures were stirred for 1 minute and then placed in a water bath for 8 hours at 298 K. The residue obtained was filtered through sintered glass (N^o. 4) and the pH of the supernatant was measured using a pH meter.

The effect of pH on the adsorption process of phenol and tyrosine by PTCa is shown in **Fig. 18**. It was noted that the adsorption is strongly dependent on the pH of the solution, it decreases with increasing pH; in fact, when the pH goes from 4 to 10, the adsorbed quantity of phenol goes from 6.35 to 2.05 mg/g and the adsorbed quantity of tyrosine also goes from 10.35 to 5.05 mg/g. These results can be interpreted by the point of zero charge pH_{ZPC} of the PTCa which is found to be 5.6: for pH values lower than 5.6, the PTCa surface becomes positively charged and the opposite for pH values higher than 5.6. As we have already seen in the study of equilibrium isotherms, the adsorption is due to an electrostatic interaction between the adsorbates and PTCa. This can be explained by the fact that phenol and tyrosine have functional groups: -OH, -NH₂ and -COOH which can be negatively charged and the surface of PTCa which can be positively charged at $pH < 5.6$. Additionally, the lower adsorption at high pH may be due to the abundance of added OH⁻ ions and, therefore, the ionic repulsion between the surface which becomes negatively charged and the phenol and tyrosine which also becomes anionic. A similar behavior has been observed previously for the adsorption of Reactive Yellow 4 on PTCa.³⁶

To describe the adsorption mechanism of different compounds in solution on apatitic tricalcium phosphate (PTCa), processes such as ion exchange, surface complexation, and dissolution followed by the precipitation of a new phase have been proposed. The mechanism by which an organic molecule is bound by PTCa strongly depends on its nature and operating conditions, such as initial concentration and pH. In this regard, the binding of phenol and tyrosine to PTCa is explained by a strong interaction between the phenolic polar groups of these compounds and the calcium ions of PTCa. Phenolic OH groups as well as NH₂ and COOH groups are often oriented toward the ionic solid (PTCa), and the hydrophobic part (aromatic core) is oriented outward. Water molecules that do not form bonds with non-polar aromatic parts are thus repelled.³⁷

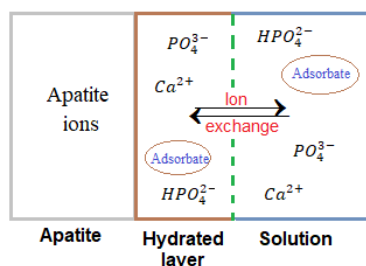


Fig. 19. Schema of the apatite/molecules interactions involving the hydrated layer of PTCa

The synthesized apatite is covered with the hydrated layer which contains relatively mobile ions (mainly Ca^{2+} , HPO_4^{2-} and PO_4^{3-}) and the previously adsorbed molecules phenolic compounds. The adsorbent/adsorbate interactions

involving the hydrated layer of apatite PTCa can be illustrated by the Schema below (**Fig. 19**). Indeed, the ions of the hydrated layer of apatite can be exchanged by ions of the solution or ionic end groups of phenolic compounds.

4. Conclusion

The interaction between PTCa and phenolic compounds in solution appears complex. It depends on several factors, such as the specific surface area (m^2/g) and the chemical composition of the adsorbent, the nature of the adsorbate (polarity and hydrophobicity), the pH of the reaction medium (isoelectric point of the adsorbate and adsorbent), incubation time, temperature, initial concentration of the adsorbate, etc. Therefore, the physicochemical properties of the examined apatite, as well as the characteristics of the incubation solution, were considered as experimental variables.

The present study shows that phenol and tyrosine can be adsorbed by apatitic tricalcium phosphate (PTCa) of $\text{Ca}/\text{P}=1.50$ with a maximum adsorption capacity of 5.56 mg/g of phenol and 9.65 mg/g of tyrosine.

The kinetic study shows equilibrium quickly obtained. The kinetics of adsorption is pseudo-second order with a good correlation between the theoretical and experimental values of the quantity of adsorbate adsorbed at equilibrium q_e .

The Langmuir model satisfactorily describes the adsorption of PTCa with a maximum adsorption capacity of 7.32 mg/g for phenol and 11.43 mg/g for tyrosine.

The adsorption is strongly dependent on the pH of the medium studied, it is important at low pH ($\text{pH}<\text{pH}_{\text{ZPC}}$) and it is weak at high pH ($\text{pH}>\text{pH}_{\text{ZPC}}$).

Additionally, adsorption also depends on temperature; the maximum adsorption capacity increased from 5.56 to 4.61 mg/g for phenol and from 9.65 to 8.75 mg/g for tyrosine, when the temperature increased from 298 to 318 K. Thermodynamic studies indicated that the adsorption process of phenol and tyrosine by PTCa was spontaneous, physisorption and exothermic in nature.

The adsorption process can be explained by the interactions between group functionals: OH, NH_2 and COOH of adsorbates studied and PTCa which may be governed by ionic bindings.

Acknowledgements

The authors thank the members of the laboratory in the Department of Chemistry at the Faculty of Sciences, Ibn Tofail University, and their own families for their support and assistance in the completion of this research topic.

References

- 1 Kasbaji M., Mennani M., Oubenali M., Ait Benhamou A., Boussetta A., Ablouh E., Mbarki M., Grimi N., El Achaby M., and Moubarik A. (2023) Bio-based functionalized adsorptive polymers for sustainable water decontamination: A systematic review of challenges and real-world implementation. *Environ. Pollut.*, 335, 15 (10) 122349.
- 2 Kasbaji M., Mennani M., Grimi N., Oubenali M., Mbarki M., EL Zakhem H., and Moubarik A. (2023) Adsorption of cationic and anionic dyes onto coffee grounds cellulose/ sodium alginate double-network hydrogel beads: Isotherm analysis and recyclability performance. *Int. J. Biol. Macromol.*, 1(6)124288.
- 3 Kasbaji M., Mennani M., Boussetta A., Grimi N., Barba F. J., and Mbarki M. (2022) Bio-adsorption performances of methylene blue (MB) dye on terrestrial and marine natural fibers: Effect of physicochemical properties, kinetic models and thermodynamic parameters. *Sep. Sci. Technol.*, 58(2) 221–240.
- 4 Kasbaji M., Mennani M., Grimi N., Barba F. J., Oubenali M., Simirgiotis M. J., Mbarki M., Moubarik A. (2022) Implementation and physico-chemical characterization of new alkali-modified bio-sorbents for cadmium removal from industrial discharges: Adsorption isotherms and kinetic approaches. *Process Biochem.*, 120 (9) 213–226
- 5 Balasooriya I. L., Chen J., Gedara S. M. K., Yingchao Han Y., and Wickramaratne M. N. (2022) Applications of Nano Hydroxyapatite as Adsorbents: A Review. *Nanomater.*, 12 (14), 2324.
- 6 Wei W., Sun R., Cui J., and Wei Z. (2010) Removal of nitrobenzene from aqueous solution by adsorption on nanocrystalline hydroxyapatite. *Desalination*, 263 (1-3) 89–96.
- 7 Dhamija M., Tyagi R., Kalra N., and Khatri A. (2022) Efficacy of Resin Infiltration and Fluoride Casein Phosphopeptide Amorphous Calcium Phosphate Varnish on Non-cavitated Active White Spot Lesions in Children: A Randomized Clinical Trial. *Pesqui. Bras. Odontopediatria Cl n. Integr.* 22 (12) e210094.
- 8 Kouar J., Ould Bellahcen T., El Amrani A., Cherif A., and Kamil N. (2021) Removal of Eriochrome Black T dye from aqueous solutions by using nanocrystalline calcium phosphate tricalcic apatitic. *Mor. J. Chem.*, 9 (4) 715-727.
- 9 El Rhilassi A., Oukass O., and Bennani-Ziatni M. (2023) Isotherms, kinetics, and thermodynamics of methionine adsorption onto poorly crystalline hydroxyapatite with different Ca/P ratios. *Curr. Chem. Lett.*, 12, 781–798.
- 10 Costa Marques R. D., Simon J., d'Arros C., Landfester K., Jurk K., and Mailänder V. (2022) Proteomics reveals differential adsorption of angiogenic platelet lysate proteins on calcium phosphate bone substitute materials. *Regen. Biomater.*, 9, rbac044.

- 11 Dalia A. A., Fatma A. S., and Hoda A. E. (2023) Kinetics and Isotherm Studies for Adsorption of Gentian Violet Dye from Aqueous Solutions Using Synthesized Hydroxyapatite. *J Environ Public Health.*, Article ID 15, 7418770.
- 12 Mourid E., EL Qor i., Benaziz L., Lakraimi M. and El khattabi E. (2018) Evaluation of the adsorption capacity of Natural Phosphate to remove Remazol Brilliant Blue R dye in aqueous solution. *Mor. J. Chem.*, 6 (3) 425-433.
- 13 Wang B., Zhang Z., and Pan H., (2023) Bone Apatite Nanocrystal: Crystalline Structure, Chemical Composition, and Architecture. *Biomimetics*, 8 (1), 90.
- 14 Zou Q., Chen H., and LI W. (2019) In vivo changes of nanoapatite crystals during bone reconstruction and the differences with native bone apatite. *Sci. Adv.*, (5) eaay6484.
- 15 Destainville A., Champion E., Bernache-Assollant D., and Laborde E. (2003) Synthesis, characterization and thermal behavior of Apatitic Tricalcium Phosphate, *Mater. Chem. Phys.*, 80 (1) 269–277.
- 16 Lagergren S., and Svenska K. (1898) About of the theory of so - called adsorption of soluble substances. *Vetenskapsakad Handl.*, 24 (2) 1-39.
- 17 Ho Y. S., and McKay G. (1999) Pseudo-second order model for sorption processes. *Process Biochem.*, 34 (5) 451- 465.
- 18 Chien S.H., and Clayton W.R. (1980) Application of Elovich Equation to the Kinetics of Phosphate Release and Sorption in Soils. *Soil. Sci. Soc. Am. J.*, 44 (2) 265-268.
- 19 Weber W. J., and Morris J. C. (1963) Kinetics of adsorption on carbon from solution. *J. Sanit. Eng. Div., Am. Soc. Civ. Eng.*, 89 (SA2) 31- 40.
- 20 El Rhilassi A., and Bennani Ziatni M. (2023) Studies of kinetic models and adsorption isotherms: application on the interaction of insulin with synthetic hydroxyapatite. *Curr. Chem. Lett.*, 12, 445–458.
- 21 Langmuir I. (1918) The adsorption of gases on plane surfaces of glass, mica and platinum. *J. Am. Chem. Soc.*, 40 (9) 1361-1403.
- 22 Freundlich H. M. F. (1906) Über die adsorption in lösungen. *Z. Phys. Chem.*, 57, 385-470.
- 23 Temkin M. J., and Pyzhev V. (1940) Recent modifications to Langmuir Isotherms. *Acta. Physicochimie USSR.*, 12, 217-222.
- 24 Dubinin M. M., and Radushkevich L. V. (1947) Equation of the Characteristic Curve of Activated Charcoal. *J. Proc. Acad. Sci. USSR, Phys. Chem.*, 55, 331-333
- 25 Weber T. W., and Chakravorti R. K. (1974) Pore and solid diffusion models for fixed-bed adsorbers. *Am. Inst. Chem. Eng. J.*, 20 (2) 228-238.
- 26 Ho Y. S. (2006) Isotherms for the sorption of lead onto peat: Comparison of linear and non-linear methods. *Pol. J. Environ. Stud.*, 15 (1) 81–86.
- 27 Jiang L., Li S., Yu H., Zou Z., Hou X., and Shen F. (2016) Amino and thiol modified magnetic multi-walled carbon nanotubes for the simultaneous removal of lead, zinc, and phenol from aqueous solutions. *Appl. Surf. Sci.*, 369, 398-413.
- 28 Hall K. R., Eagleton L. C., Acrivos A., and Vermeulen T. (1966) Pore- and solid-diffusion kinetics in fixed-bed adsorption under constant-pattern conditions. *Ind. Eng. Chem. Fund.*, 5(2) 212-223.
- 29 Helfferich F. (1962) Ion exchange. *McGraw-Hill, New York*, 335-360.
- 30 El Rhilassi A., and Bennani Ziatni M., (2022) Experimental study on the interaction of insulin with apatitic calcium phosphates analogous to bone mineral: adsorption and release. *Curr. Chem. Lett.*, 11, 341–352.
- 31 Ho Y.S. (2006) Isotherms for the sorption of lead onto peat : Comparison of linear and non-linear methods. *P. J. Env. Studies*, 15, 81–86.
- 32 Al-Anber Z.A., and Matouq M.A.D. (2008) Batch adsorption of cadmium ions from aqueous solution by means of olive cake. *J. Hazard. Mater.*, 151, 194–201.
- 33 Jiang L., Li S., Yu H., Zou Z., Hou X., Shen F., Li C., and Yao X. (2016) Amino and thiol modified magnetic multiwalled carbon nanotubes for the simultaneous removal of lead, zinc, and phenol from aqueous solutions. *Appl. Surf. Sci.*, 369, 398–413.
- 34 Hameed B. H., Ahmad A. A., and Aziz N. (2007). Isotherms, kinetics and thermodynamics of acid dye adsorption on activated palm ash. *Chem. Eng. J.*, 133 (1-3) 195–203.
- 35 Singh T.S., and Pant K.K. (2004) Equilibrium, Kinetics and Thermodynamic Studies for Adsorption of As (III) on Activated Alumina. *Sep. Pur. Technol.*, 36 (2) 139–147.
- 36 El Boujaady H., Mourabet M., El Rhilassi A., Bennani-Ziatni M., El Hamri R., and Taitai A. (2017) Interaction of adsorption of reactive yellow 4 from aqueous solutions onto synthesized calcium Phosphate. *J. Saudi Chem. Soc.*, 21, S94–S100.
- 37 Lemlikchi O., Fiallo M., Scharrock P., Nzihou A., and Mecherrri M.O. (2012) Treatment of textile waste waters by hydroxyapatite co-precipitation with adsorbent regeneration and reuse. *Waste and Biomass Valor.*, 3(1) 75-79.

